Water Research 85 (2015) 286–294

Contents lists available at ScienceDirect

Water Research

journal homepage: www.elsevier.com/locate/watres

# Tracking changes in the optical properties and molecular composition of dissolved organic matter during drinking water production

E.E. Lavonen [a, *], D.N. Kothawala [a, b], L.J. Tranvik [b], M. Gonsior [c, d], P. Schmitt-Kopplin [e, f], S.J. Köhler [a]

[a] Department of Aquatic Sciences and Assessment, Swedish University of Agricultural Sciences (SLU), 75007, Uppsala, Sweden
[b] Department of Ecology and Genetics/Limnology, Uppsala University, 75236, Uppsala, Sweden
[c] Department of Thematic Studies, Unit of Environmental Change, Linköping University, 58183, Linköping, Sweden
[d] Chesapeake Biological Laboratory, University of Maryland Center for Environmental Science, Solomons, MD 20688, USA
[e] Analytical BioGeoChemistry, German Research Center for Environmental Health, Helmholtz Zentrum München, 85764, Neuherberg, Germany
[f] Analytical Food Chemistry, Technische Universität München, 85354, Freising-Weihenstephan, Germany

ARTICLE INFO

*Article history:*
Received 14 April 2015
Received in revised form
10 August 2015
Accepted 14 August 2015
Available online 28 August 2015

*Keywords:*
Dissolved organic matter
Drinking water
Absorbance
Fluorescence
FT-ICR-MS

ABSTRACT

Absorbance, 3D fluorescence and ultrahigh resolution electrospray ionization Fourier transform ion cyclotron resonance mass spectrometry (ESI-FT-ICR-MS) were used to explain patterns in the removal of chromophoric and fluorescent dissolved organic matter (CDOM and FDOM) at the molecular level during drinking water production at four large drinking water treatment plants in Sweden. When dissolved organic carbon (DOC) removal was low, shifts in the dissolved organic matter (DOM) composition could not be detected with commonly used DOC-normalized parameters (e.g. specific $UV_{254}$ absorbance – SUVA), but was clearly observed by using differential absorbance and fluorescence or ESI-FT-ICR-MS. In addition, we took a novel approach by identifying how optical parameters were correlated to the elemental composition of DOM by using rank correlation to connect optical properties to chemical formulas assigned to mass peaks from FT-ICR-MS analyses. Coagulation treatment selectively removed FDOM at longer emission wavelengths (450–600 nm), which significantly correlated with chemical formulas containing oxidized carbon (average carbon oxidation state $\geq$0), low hydrogen to carbon ratios (H/C: average ± SD = 0.83 ± 0.13), and abundant oxygen-containing functional groups (O/C = 0.62 ± 0.10). Slow sand filtration was less efficient in removing DOM, yet selectively targeted FDOM at shorter emission wavelengths (between 300 and 450 nm), which commonly represents algal rather than terrestrial sources. This shorter wavelength FDOM correlated with chemical formulas containing reduced carbon (average carbon oxidation state $\leq$0), with relatively few carbon-carbon double bonds (H/C = 1.32 ± 0.16) and less oxygen per carbon (O/C = 0.43 ± 0.10) than those removed during coagulation. By coupling optical approaches with FT-ICR-MS to characterize DOM, we were for the first time able to confirm the molecular composition of absorbing and fluorescing DOM selectively targeted during drinking water treatment.



## 1. Introduction

Dissolved organic matter (DOM) in inland waters is a complex, heterogeneous mixture of natural organic compounds of both terrigenous and aquatic origin. These compounds vary in size, hydrophobicity, age, bioavailability and reactivity (Steinberg et al., 2008; Thurman, 1985). In Sweden, as in several other countries in Northern Europe and North America, dissolved organic carbon (DOC) concentrations, commonly used as a proxy for DOM abundance, are currently increasing in surface waters (Evans et al., 2005; Freeman et al., 2001; Ledesma et al., 2012; Roulet and Moore, 2006). Because colored DOM in particular has been found to increase (Hongve et al., 2004), this is often referred to as browning of inland waters (Roulet and Moore, 2006). It is presently unclear whether DOC concentrations will stabilize or continue to increase in the future, and which changes in its composition may occur.

* Corresponding author.
*E-mail address:* elin.lavonen@slu.se (E.E. Lavonen).

http://dx.doi.org/10.1016/j.watres.2015.08.024

Surface water is a major source of drinking water. Because the increasing DOM levels were not considered when many water treatment plants (WTPs) were constructed, the industry is currently struggling to manage sufficient DOM removal in order to maintain a high drinking water quality. Rising DOC concentrations in raw waters increase the demand on treatment and becomes costly due to the need for higher doses of chemical coagulants (Eikebrokk et al., 2004), and more frequent regeneration of active carbon filters and cleaning of membrane surfaces. Residual DOM results in the consumption of disinfectants (such as chlorine chemicals and UV) and leads to production of disinfection by-products (Richardson, 2011; Richardson et al., 2007) as well as fouling of costly membranes and active carbon filters (Kaiya et al., 1996; Summers et al., 1989). Besides the obvious economic implications, disinfection by-products may pose health risks (Richardson, 2011; Richardson et al., 2007). Recently, many (so far structurally unknown) disinfection by-product components have been identified (Gonsior et al., 2014; Lavonen et al., 2013; Zhang et al., 2012a, 2012b), which may also contribute to negative health effects. Low DOC concentration in drinking water is further desirable to avoid potential regrowth of microorganisms in the distribution system (Camper, 2004; Huck, 1990), as well as for esthetic reasons (color, odor and taste).

WTPs use a range of treatment techniques to remove DOM, including chemical coagulation and slow sand filtration. Coagulant dosing is optimized with respect to a number of parameters such as turbidity, color or DOC removal and residual iron or aluminum. The DOC removal efficiency may vary greatly between WTPs even when their treatment processes are similar. The range of removal efficiencies has been reported to occur due to differences in DOM quality (e.g. (Matilainen et al., 2010; Ødegaard et al., 2010). Yet, detailed information regarding selective DOM removal is sparse, and highly needed to improve our ability to predict treatability of different raw waters and to develop more efficient treatment strategies. Only a few studies have addressed the selective removal of DOM caused by coagulation at the molecular level (Gonsior et al., 2014; Zhang et al., 2012a).

Because DOM removal is costly, there is an increasing demand for online monitoring techniques to track temporal changes in DOM quality of relevance to the operation of WTPs. Many WTPs depend solely on the DOC-normalized value of absorbance at 254 nm (specific UV absorbance – SUVA) to assess DOM quality. SUVA is an indicator of carbon aromaticity (Weishaar et al., 2003) and has been shown to be useful to assess the removal efficiency of DOM with coagulation (Matilainen et al., 2011). SUVA provides an estimate of the average aromatic content for all DOM compounds present in solution (Traina et al., 1990; Weishaar et al., 2003). However, samples with the same SUVA may differ in their distribution around this average value (Shutova et al., 2014), and consequently in their reactivity. Due to the complexity of DOM, more detailed and sensitive analytical approaches are likely to provide more insight regarding DOM reactivity. Fluorescence spectroscopy is a promising alternative because it is a rapid and straightforward analytical technique, and still provides detailed information. When applied in 3D mode, it generates an emission-excitation matrix (EEM), providing a fingerprint of the fluorescent DOM (FDOM) in a sample, which can supply substantial information about DOM quality. The method therefore holds strong advantages for more detailed offline or online monitoring. A key limitation of fluorescence is the lack of molecular level information. Hence, combining fluorescence spectroscopy with a method that provides detailed molecular level information is needed to identify how optical properties are related to the molecular characteristics. Changes in measured fluorescence EEMs and calculated indices during treatment processes used in drinking water production are commonly small. Differential fluorescence may however capture these small changes and has previously been applied to investigate e.g. the formation of several DBPs (at a single excitation wavelength) (Roccaro et al., 2009), removal of PARAFAC components during coagulation (Sanchez et al., 2013), as well as removal of different fluorophores during ozonation of a wastewater effluent (Liu et al., 2015). In this study, we used differential fluorescence of full EEMs in order to identify potential patterns in the removal of FDOM during conventional drinking water treatment and develop a novel index related to FDOM reactivity.

ESI-FT-ICR-MS provides ultrahigh mass resolution and has a mass accuracy below 1 ppm and is therefore able to differentiate between DOM components having small differences in molecular mass. To date, only a few studies have coupled results from FT-ICR-MS analysis with fluorescence spectra (Gonsior et al., 2013; Herzsprung et al., 2012; Kellerman et al., 2014; Stubbins et al., 2014) and none during drinking water production. We aimed to investigate the molecular composition of FDOM and CDOM that is targeted during conventional drinking water treatment processes by correlating conventional and novel optical indices with individual DOM components from FT-ICR-MS analyses. Through this approach, we evaluate the usefulness of commonly used optical indices to describe selective DOM removal and couple DOM reactivity to specific chemical properties.

## 2. Methods

### 2.1. Sampling

Water samples were collected from four Swedish WTPs; Lovö, Lackarebäck, Ringsjö, and Kvarnagården (Fig. A1) on a monthly to bi-monthly basis between May and December 2011. Lovö WTP was sampled between all the main treatment process steps, namely alum ($Al_2(SO_4)_3$) coagulation, slow sand filtration, and disinfection with UV and monochloramine ($NH_2Cl$). The three additional WTPs were sampled at the raw water intake and the outgoing treated drinking water. Ringsjö WTP applies $FeCl_3$ coagulation, slow sand filtration and sodium hypochlorite (NaOCl) disinfection. Lackarebäck WTP uses pre-chlorination ($Cl_2$), $Al_2(SO_4)_3$ coagulation, active carbon filtration, and disinfection with $Cl_2$ and $ClO_2$. At Kvarnagården WTP only rapid sand filtration is applied to reduce the water turbidity before disinfection using $NH_2Cl$ and UV (Fig. A2).

All samples were analyzed for DOC, UV-Vis absorbance, and 3D fluorescence. Prior to these analyses, samples were filtered (within 24 hrs after sampling) using pre-rinsed (Milli-Q, 18.2 Ω $cm^{-1}$) 0.45 μm cellulose acetate filters (Minisart, Sartorius). During one sampling event (October 17–18, 2011) samples were also collected for FT-ICR-MS analyses.

### 2.2. Analyses and data processing

#### 2.2.1. DOC and UV-Vis absorbance

Filtered samples were acidified to pH 2 with 2 M HCl and analyzed for DOC, after purging of inorganic carbon with $CO_2$-free air, using a Shimadzu TOC-$V_{CPH}$ carbon analyzer. Absorbance spectra were recorded between 240 and 600 nm in a spectrophotometer (Perkin-Lambda 40) in a 1 cm quartz cuvette for samples at ambient pH. For further details see Lavonen et al., 2013. Specific absorbance (SUVA) was calculated using the absorbance at 254 nm normalized to the DOC concentration and is reported in the unit liter per milligram carbon and meter (L $mg^{-1}$ $m^{-1}$) (Weishaar et al., 2003). Differential absorbance spectra were calculated by subtracting the measured absorbance after a

treatment process from that before. For values below 0.02 $cm^{-1}$, which occurred at wavelengths >320 nm for the treated waters, differential absorbance spectra could not be determined, because the signal to noise ratio was too low (defined as fluctuations being larger than the value of the calculated differential signal), and therefore only wavelengths up to 320 nm were used.

### 2.2.2. 3D fluorescence

Fluorescence EEMs (excitation (ex) 250–445 nm, 5 nm intervals, emission (em) 300–600 nm, 4 nm intervals) were measured on filtered samples using a Fluoromax-2 spectrofluorometer (Horiba Jobin Yvon). Additional details on the measurement settings have been previously described (Kothawala et al., 2014). All EEMs were corrected i) through blank subtraction (MilliQ water, 18.2 Ω $cm^{-1}$) to reduce scatter from the water Raman peak, ii) for instrument/spectral biases according to the emission and excitation correction factors provided by the manufacturer, iii) for primary and secondary inner filter effects using the absorbance spectra (Kothawala et al., 2013; Lakowicz, 2007; MacDonald et al., 1997), and iv) by nullifying signal intensities in regions where first and second order Rayleigh scattering appeared. The corrected EEMs were converted from counts per second (cps) to water Raman units (R.U.) by dividing each data point with the area under the water Raman peak (ex = 350 nm, em = 380–420 nm) (Lawaetz and Stedmon, 2009).

3D fluorescence data was used to calculate three previously established indices; humification index (HIX = ratio of areas under the emission curve at 435–480 nm and 300–345 nm plus 435–480 nm at an excitation wavelength 254 nm) (Ohno, 2002), fluorescence index (FI = emission intensity at 470 nm divided with that of 520 nm at 370 nm excitation) (Cory and McKnight, 2005) and freshness index (β:α = ratio of emission intensity at 380 nm and maximum intensity between 420 and 435 nm at an excitation wavelength of 310 nm) (Parlanti et al., 2000). The indices have been coupled to degree of humification (higher HIX = more humified material), source (a gradient from microbial (FI ≈ 1.8) to terrestrial (FI ≈ 1.3)) and age (high freshness index = larger contribution of more freshly produced DOM) respectively.

Differential EEMs (ΔEEMs) were calculated as follows (provided conceptually in Fig. 1):

$$\Delta\text{EEM} = \text{EEM of removed FDOM}: \quad \Delta EEM = EEM_{before} - EEM_{after}$$

$$\text{Removed fraction}(\%): \quad EEM_{\%removed} = \frac{\Delta EEM}{EEM_{before}}$$

Normalized ΔEEM ($\Delta EEM_{normalized}$):

1) $EEM_{normalized} = \frac{EmI_{Ex\lambda,\ Em\lambda}}{EmI_{max}}$ (for all excitation emission pairs)
2) $\Delta EEM_{normalized} = EEM_{normalized\ 1} - EEM_{normalized\ 2}$

where $EmI_{Ex\lambda,Em\lambda}$ is the emission intensity at any given excitation emission wavelength pair and $EmI_{max}$ is the maximum emission intensity for the measured EEM. The difference in pH for samples used for calculations of ΔEEMs were within 0.8 pH units and the majority within 0.5 pH units which should minimize the possibility of patterns occurring due to pH effects. Indices were calculated for the ΔEEMs in the same manner as for the measured samples. DOM removal during slow sand filtration was limited and the calculated signal intensities for the ΔEEMs were affected by noise. Therefore, the excitation spectra at 254 (HIX), 310 (β:α) and 370 nm (FI) were smoothed using a Savitzky-Golay filter (Savitzky and Golay, 1964) before index calculation (Fig. A3).

In a novel approach, we calculated the relative intensity of total fluorescence (%FDOM) across three regions of the EEM based on emission wavelength, at long (%$FDOM_{450\text{-}600}$: 450–600 nm), medium (%$FDOM_{350\text{-}450}$: 350–450 nm) and short (%$FDOM_{300\text{-}350}$: 300–350 nm) emission wavelengths. The regions were selected to capture the most distinct removal occurring during treatment with coagulation (Em > 450 nm) and slow sand filtration (Em < 450 nm) (Fig. 1). The shorter emission wavelength region was further divided in order to see if changes in the region where protein-like fluorescence occurs (Em < 350 nm (Coble et al., 1998, 1990)) could be detected.

### 2.2.3. FT-ICR-MS

Samples for FT-ICR-MS analysis were filtered using Whatman GF/F glass fiber filters, acidified to pH 2, and the DOM was extracted using Agilent Bond Elut PPL solid-phase extraction cartridges (1 g of polar functionalized polystyrene divinylbenzene (PPL)) according

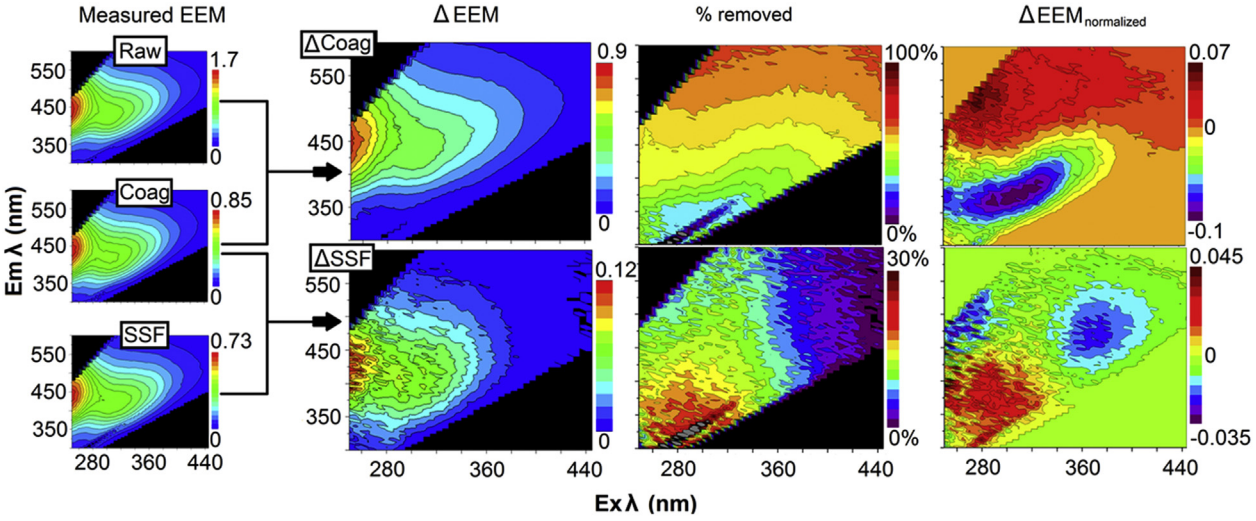


**Fig. 1.** Calculation scheme for differential EEMs during $Al_2(SO_4)_3$ coagulation (ΔCoag, top row) and slow sand filtration (ΔSSF, bottom row) at Lovö WTP where ΔEEMs are the differential EEMs, %removed demonstrate the removed fraction and $\Delta EEM_{normalized}$ are the differential EEMs calculated from EEMs that has been normalized using the maximum fluorescence intensity.

to (Dittmar et al., 2008). The adsorption efficiency (defined as the difference in DOC concentration before and after extraction) was 74 ± 7% (Lavonen et al., 2013).

The extracted samples were analyzed at the Helmholtz Center for Environmental Health in Munich, Germany using a Bruker Solarix 12 T FT-ICR mass spectrometer with electrospray ionization (Apollo II). Mass resolution was 1,000,000 for m/z = 200, 500,000 for m/z = 400 and, 350,000 for m/z = 600. Arginine and its specific mass peaks (m/z = 173.10440, 347.21607, 521.32775 and 695.43943 for singly negatively charged ions) were used for external calibration. To further improve the precision, internal calibration was also performed using known exact mass peaks that are always present in DOM samples (Table A1) (Gonsior et al., 2011). Chemical formulas were assigned to the mass peaks according to $^{12}C_{0\text{-}100}$, $^{16}O_{0\text{-}80}$, $^{1}H_{0\text{-}\infty}$, $^{32}S_{0\text{-}32}$, $^{14}N_{0\text{-}2}$, $^{35}Cl_{0\text{-}3}$ and $^{13}C_{0\text{-}1}$ and the following criteria were applied: i) mass accuracy <0.7 ppm, and ii) peak intensity >5,000,000. On average, approximately 15,000 peaks were identified in each sample, of which roughly 20% met the above stated criteria and could be assigned unequivocal chemical formulas. In this study, we focused on formulas containing only C, H and O, because nitrogen- and sulfur-containing compounds showed only low abundances, in agreement with a previous study (Gonsior et al., 2013). Detailed information regarding extraction, data processing, limitations, and calculations can be found in a previous study, analyzing chlorine-containing organic components in the same samples (Lavonen et al., 2013).

Samples from Lovö WTP were taken in duplicate to assure high data quality. One of the duplicate samples from the rapid sand filtrate deviated systematically in signal intensities and was therefore not included. For the remaining samples we performed a hierarchical cluster analysis (HCA) using Ward's method (Fig. A4). Because the results from the HCA showed that no difference could be quantified between the rapid sand filtrate and the slow sand filtrate, no results are presented from the slow sand filtration process.

Signal intensities of all individual m/z peaks were normalized using the most abundant m/z peak in each mass spectrum to obtain relative abundances. Changes in relative abundance are described in percentage points (relative abundance in one sample minus the relative abundance in the other sample). Differences in relative abundance between duplicate samples were, on average, 0.9 ± 1.5 percentage points. Therefore, when comparing two samples, only differences in relative abundance that exceeded 2.5 percentage points were considered significant. Ratios of O/C and H/C as well as double bond equivalency per carbon (DBE/C) and the average carbon oxidation state ($\overline{C_{OS}}$) (Kroll et al., 2011; Lavonen et al., 2013) were calculated.

#### 2.2.4. Statistics

We examined positive correlations between SUVA, HIX, FI, β:α, %$FDOM_{450\text{-}600}$, %$FDOM_{350\text{-}450}$, %$FDOM_{300\text{-}350}$ and the relative abundance of CHO formulas assigned to FT-ICR-MS data using rank correlation according to (Herzsprung et al., 2012). All CHO formulas present in at least 10 out of the 11 samples were included, resulting in 857 components in total.

The significance of changes in DOC concentration and composition during treatment was obtained using two-tailed Student's paired t-tests.

## 3. Results & discussion

We will first present results from the rank correlation in order to identify patterns in correlated chemical formulas between different commonly used (SUVA, HIX, FI and β:α) and novel (%$FDOM_{300\text{-}350}$, %$FDOM_{350\text{-}450}$, %$FDOM_{450\text{-}600}$) optical spectroscopic indices. This information will then be used in a novel approach to understand how representative changes in spectroscopic indices are for the shift in molecular level composition during different conventional drinking water processes, namely coagulation with $Al_2(SO_4)_3$, slow sand filtration, and disinfection with UV and $NH_2Cl$. We will, for the first time, identify chemical features for SUVA and FDOM that can be related to DOM oxidative reactivity. Lastly, we will use normalized differential EEMs to explain differences in the coagulation treatability of different raw waters.

### 3.1. Correlations between optical spectroscopic parameters and chemical formulas

Several of the spectroscopic indices correlated similarly to individual CHO components (Table A3), clearly separating them into two groups (A–D and E–G in Fig. 2). One group included SUVA, HIX, and %$FDOM_{450\text{-}600}$ and the other FI, β:α, %$FDOM_{300\text{-}350}$ and %$FDOM_{350\text{-}400}$. The two groups will hereafter be referred to as terrestrial and in-lake produced DOM indicators in accordance with previously established relationships between the indices, fluorescence regions and DOM source (Kothawala et al., 2014; McKnight et al., 2001; Parlanti et al., 2000; Zsolnay et al., 1999). Out of the 857 CHO-formulas that were included in the rank correlation, 632 were significantly positively correlated ($p < 0.05$) to one or more optical spectroscopic parameters.

Within the group of terrestrial DOM indicators, 208 CHO formulas correlated with both SUVA and %$FDOM_{450\text{-}600}$, which equaled 90% and 98% of the total amount of positively correlated formulas respectively (Fig. 2F&G, Fig. A5, Table A2). These formulas had, on average, high O/C (0.63 ± 0.09) and DBE/C (0.64 ± 0.07) (Table A3). 79 of these CHO formulas also correlated with HIX (Fig. 2E, Fig. A5). HIX was furthermore uniquely correlated to 36 formulas with even higher average O/C (0.72 ± 0.09) and lower DBE/C (0.50 ± 0.05) (Table A3). Out of all the CHO components that were coupled to these three measures, all but 1 had an average carbon oxidation state ≥0 (Fig. 3, Table A4). SUVA has earlier been shown to be positively correlated with aromaticity measured with $^{13}$C-NMR (Weishaar et al., 2003), indicating that a significant amount of the CHO components correlating with the terrestrial indicators correspond to aromatic compounds, as would be expected because they originate from structural plant and animal residues, e.g. lignin. The relatively high oxygen content of the components indicates a prevalence of oxygen-containing functional groups, a feature that is connected to the humification process where hydrophobic soil organic matter is solubilized through the addition of e.g. hydroxyl and carboxyl groups (Kleber and Johnson, 2010).

For the in-lake produced DOM indicators, 277 chemical formulas correlated with all four parameters, i.e., FI, β:α, %$FDOM_{350\text{-}450}$ and %$FDOM_{300\text{-}350}$, representing 81–95% of the total amount of formulas that were positively correlated to the four individual spectroscopic measures (Fig. A5, Table A2). All in-lake produced DOM indicators are based on a shift in fluorescence emission maximum towards shorter wavelengths, which could be attributed to i) reduction in the length of the π-electron system caused by e.g. a decrease in the number of aromatic rings or, ii) removal of e.g. carbonyl and hydroxyl functional groups (Coble, 1996; Senesi, 1990). Consequently, the 277 molecular formulas had relatively low O/C (0.43 ± 0.10) and DBE/C (0.39 ± 0.08) (Table A3) compared to the terrestrial components. Out of all 359 formulas coupled to any of these four measures (FI, β:α, %$FDOM_{350\text{-}450}$ and %$FDOM_{300\text{-}350}$), all but one had an average carbon oxidation state≤0 (Fig. 3, Table A4). These results indicate that carbon oxidation is an important chemical feature related to DOM source, separating terrestrial and in-lake produced DOM into oxidized and reduced components respectively.

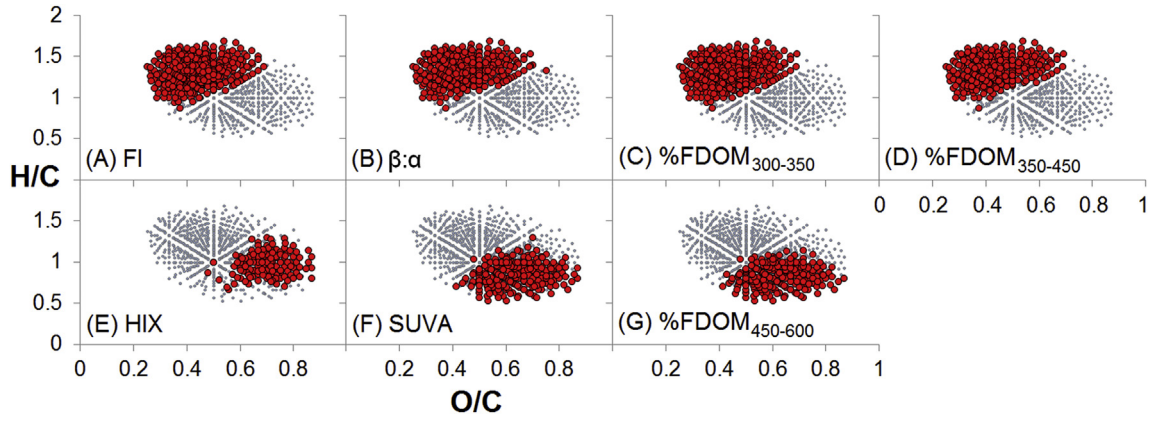


**Fig. 2.** van Krevelen diagrams demonstrating relationships between optical spectroscopic parameters and individual chemical formulas for components containing C, H and O. Red points show the position of positively correlated formulas ($p < 0.05$) in the van Krevelen space (x-axis showing the oxygen to carbon ratio and the y-axis the hydrogen to carbon ratio). Gray points represent formulas without significant correlation. (A) fluorescence index, (B) freshness index, (C) %FDOM with emission between 300 and 350 nm, (D) %FDOM with emission between 350 and 450 nm, (E) humification index, (F) specific UV absorbance (254 nm), and (G) %FDOM with emission between 450 and 600 nm. (For interpretation of the references to color in this figure legend, the reader is referred to the web version of this article.)

### 3.2. Selective DOM removal

#### 3.2.1. Coagulation

The largest reduction in DOC concentration at Lovö WTP of approximately 40% occurred during the coagulation process (Table 1). This was expected because the removal efficiency with $Al_2(SO_4)_3$ coagulation for waters in the SUVA range 2–4 have been reported to be 25–50% (Edzwald, 1993; Matilainen et al., 2010). Coagulation selectively removed chromophoric DOM (CDOM), as demonstrated by a decrease in the sum of absorbance per DOC (TotAbs/DOC) and SUVA (Table 1). Fluorescent DOM (FDOM) was also targeted during coagulation, as shown by a decrease in the total fluorescence per DOC (TotFDOM/DOC) (Table 1). The removal of FDOM increased with emission wavelength (Fig. 1). Accordingly, $\%FDOM_{450\text{-}600}$ and HIX decreased while FI and β:α increased (Table 1). The change in FDOM character during coagulation was accentuated for the indices obtained from ΔEEMs (Fig. 4), with relatively high HIX (0.94 ± 0.01) and low β:α (0.47 ± 0.02) and FI (1.27 ± 0.03) close to the reported terrestrially derived end member (approximately 1.3) (Cory and McKnight, 2005; Cory et al., 2007; McKnight et al., 2001). Chemical formulas of DOM that decreased in abundance upon coagulation had relatively high O/C and low H/C and the majority of assigned formulas had a positive average carbon oxidation state (Fig. 5A). All our independent spectroscopic measures demonstrated that coagulation is a highly selective process in the drinking water treatment and removes DOM with characteristics typically associated with terrestrial organic matter. Targeted removal of terrestrial DOM with high O/C ratios during coagulation is well known and has been demonstrated in a number of previous studies utilizing various analytical techniques (e.g. (Baghoth et al., 2011; Bieroza et al., 2009a, b; 2010, Edzwald, 1993; Gonsior et al., 2014; Sanchez et al., 2013; Shutova et al., 2014; Volk et al., 2000; Zhang et al., 2012a). Almost all (99%) of the CHO components that correlated with SUVA and $\%FDOM_{450\text{-}600}$ were found to decrease during coagulation, which demonstrate the usefulness of the two spectroscopic measures for describing coagulation treatability. $\%FDOM_{450\text{-}600}$ was, however, a more sensitive measure than SUVA, allowing the detection of changes in DOM character even when DOC removal was small, i.e. during slow sand filtration (Table 1) (see section 3.2.2). We suggest $\%FDOM_{450\text{-}600}$ to be a useful single parameter to use at WTPs to capture changes in the DOM composition, and assess the treatability during coagulation. Nevertheless, SUVA and $\%FDOM_{450\text{-}600}$ may not fully capture the chemical components targeted by coagulation as formulas coupled to the in-lake produced DOM indicators also decreased during the treatment (Table A5). Looking at the most pronounced shifts in composition, 176 components decreased in relative abundance by more than 5 percentage points during coagulation and out of those 80% correlated with the terrestrial indicators and only 5% with the in-lake produced DOM indicators. This pattern is in agreement with the observed gradient in FDOM removal from approximately 30% for shorter-emission wavelengths (<350 nm) up to 55–60% for longer emission wavelengths (500–600 nm) (Fig. 1). The removal of FDOM is in coherence with a previous study (Sanchez et al., 2013) and show that similar results can be obtained by calculating the removed fraction of FDOM from measured EEMs compared to from PARAFAC components modeled from ΔEEMs as applied by Sanchez et al. (2013). In general, we found that all spectroscopic parameters connected to terrestrial DOM provided a good estimation of the DOM treatability during coagulation, in line with the high selectivity of the treatment towards oxidized components (Fig. 5A). Nonetheless, changes in the indices only provide

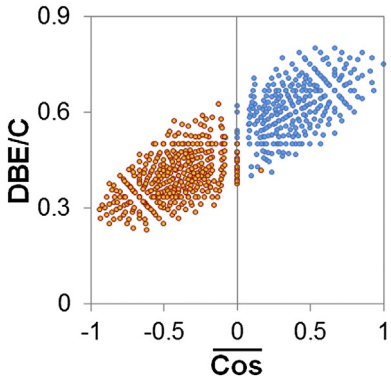


**Fig. 3.** Double bond equivalency per carbon (DBE/C) and the average carbon oxidation state ($\overline{C_{OS}}$) of chemical formulas containing C, H and O that correlated with terrestrial indicators (humification index, specific UV absorbance (254 nm) and % FDOM with emission between 450 and 600 nm) (blue points) and those correlated to in-lake produced DOM indicators (fluorescence index, freshness index, %FDOM with emission between 300 and 350 nm, and %FDOM with emission between 350 and 450 nm) (orange points). The two groups are clearly separated by an average carbon oxidation state equal to zero. (For interpretation of the references to color in this figure legend, the reader is referred to the web version of this article.)

**Table 1**
Mean values (±SD) of dissolved organic carbon (DOC) concentration and spectrophotometric parameters. Lo = Lovö, Kv = Kvarnagården, La = Lackarebäck and Ri = Ringsjö water treatment plants (WTPs). Surf = surface water, Raw = raw water at the WTPs intake, Raw/mix = raw water mixed with groundwater (1/4 groundwater for Kv and 1/8 for Ri), RSF = rapid sand filtrate, sample taken after coagulation and rapid sand filtration, SSF = slow sand filtrate, Drink = outgoing drinking water, sampled after disinfection. DOC = dissolved organic carbon concentration, SUVA = specific UV absorbance at 254 nm, TotFDOM/DOC = sum of fluorescence intensities divided by DOC concentration, TotAbs/DOC = sum of absorbance intensities divided by DOC concentration, $\%FDOM_{450\text{-}600}$ = sum of fluorescence intensities with emission between 450 and 600 nm divided by the full emission wavelength range (300–600 nm), HIX = humification index, FI = fluorescence index, and β:α = freshness index.

| WTP | Sample | n | DOC (mg $L^{-1}$) | SUVA (L $mg^{-1}$ $m^{-1}$) | TotFDOM/DOC (R.U. L $mg^{-1}$) | TotAbs/DOC (L $mg^{-1}$ $cm^{-1}$) | $\%FDOM_{450\text{-}600}$ | $\%FDOM_{350\text{-}450}$ | $\%FDOM_{300\text{-}350}$ | HIX | FI | β:α |
|---|---|---|---|---|---|---|---|---|---|---|---|---|
| Lo | Raw | 10 | 8.9 ± 0.4 | 2.7 ± 0.11 | 113.8 ± 13.4 | 2.0 ± 0.12 | 53.3 ± 0.5 | 44.0 ± 0.4 | 2.6 ± 0.2 | 0.90 ± 0.01 | 1.41 ± 0.02 | 0.61 ± 0.01 |
| | RSF | 8 | 5.1 ± 0.3*** | 1.9 ± 0.15*** | 95.2 ± 9.7** | 1.4 ± 0.14*** | 48.7 ± 0.6*** | 47.6 ± 0.4*** | 3.7 ± 0.2*** | 0.87 ± 0.02*** | 1.58 ± 0.03*** | 0.74 ± 0.01*** |
| | SSF | 8 | 4.7 ± 0.3** | 1.9 ± 0.12 | 100.2 ± 16.1 | 1.4 ± 0.14 | 50.0 ± 0.5*** | 46.5 ± 0.4*** | 3.6 ± 0.4 | 0.87 ± 0.02 | 1.57 ± 0.01 | 0.72 ± 0.01** |
| | Drink | 10 | 4.4 ± 0.3 | 1.9 ± 0.15 | 107.8 ± 20.7 | 1.4 ± 0.12 | 50.3 ± 0.5 | 46.2 ± 0.2 | 3.4 ± 0.5* | 0.88 ± 0.02 | 1.56 ± 0.01 | 0.72 ± 0.01 |
| Kv | Surf | 8 | 3.3 ± 0.2 | 2.9 ± 0.36 | 103.7 ± 18.8 | 2.5 ± 0.52 | 56.9 ± 0.7 | 40.3 ± 0.2 | 2.8 ± 0.6 | 0.87 ± 0.03 | 1.38 ± 0.02 | 0.54 ± 0.01 |
| | Raw/mix | 8 | 3.0 ± 0.2** | 2.8 ± 0.41* | 101.5 ± 16.6 | 2.4 ± 0.48 | 56.5 ± 0.5 | 40.7 ± 0.2** | 2.8 ± 0.5 | 0.87 ± 0.02 | 1.39 ± 0.02 | 0.54 ± 0.01 |
| | Drink | 8 | 3.0 ± 0.3 | 2.5 ± 0.42** | 110.6 ± 22.7 | 2.2 ± 0.45 | 56.9 ± 0.5 | 40.5 ± 0.2 | 2.7 ± 0.5 | 0.88 ± 0.02 | 1.41 ± 0.02 | 0.54 ± 0.01 |
| La | Raw | 6 | 5.2 ± 0.2 | 3.0 ± 0.13 | 96.9 ± 8.9 | 2.4 ± 0.14 | 55.6 ± 0.5 | 41.5 ± 0.3 | 2.9 ± 0.3 | 0.88 ± 0.01 | 1.36 ± 0.02 | 0.55 ± 0.01 |
| | Drink | 6 | 2.4 ± 0.2*** | 1.5 ± 0.04*** | 64.5 ± 20.5** | 1.3 ± 0.35** | 46.4 ± 1.0*** | 47.6 ± 0.7*** | 6.0 ± 1.7** | 0.77 ± 0.05*** | 1.63 ± 0.04*** | 0.79 ± 0.01*** |
| Ri | Raw/mix | 7 | 10.1 ± 0.3 | 4.0 ± 0.17 | 133.8 ± 19.9 | 3.5 ± 0.17 | 59.1 ± 0.4 | 39.2 ± 0.3 | 1.6 ± 0.1 | 0.93 ± 0.00 | 1.34 ± 0.01 | 0.48 ± 0.01 |
| | Drink | 7 | 2.7 ± 0.3*** | 1.5 ± 0.24*** | 98.9 ± 23.6* | 1.1 ± 0.19*** | 50.5 ± 0.3*** | 46.0 ± 0.3*** | 3.5 ± 0.5*** | 0.85 ± 0.01*** | 1.63 ± 0.02*** | 0.68 ± 0.01*** |

***p < 0.0001, **p < 0.01, *p < 0.05, significance of change (paired two-tailed Student's t-test) compared to the sample taken closest before in the treatment train.




**Fig. 4.** Mean values (±SD) of indices (FI = fluorescence index, β:α = freshness index, HIX = humification index) calculated from differential excitation emission matrices for $Al_2(SO_4)_3$ coagulation (gray) (n = 7) and slow sand filtration (white) (n = 2/5/4 for FI/β:α/HIX) at Lovö WTP.

information about which type of DOM that is preferentially removed and cannot capture the range of removal from FDOM with shorter to longer emission wavelengths and both components connected to terrestrial and in-lake produced DOM. Differential EEMs, on the other hand, render a more complete picture of the range of removal efficiencies across DOM with different fluorescence characteristics, as does FT-ICR-MS analysis for individual chemical components.

### 3.2.2. *Slow sand filtration*

In the biological sand filters at Lovö WTP, there was a small but significant removal of DOC (8 ± 3%, p = 0.003) (Table 1). As opposed to coagulation, the slow sand filters had no significant effect on




**Fig. 5.** Change in relative abundance of chemical formulas containing C, H and O that was present both before and after a treatment. Left side = van Krevelen diagrams for CHO formulas where bubble size represents the change in relative abundance during the coagulation and disinfection processes (colored bubble = increase, white bubble = decrease), right side = change in relative abundance as a function of the average carbon oxidation state ($\bar{C}_{OS}$). (A) $Al_2(SO_4)_3$ coagulation, Lovö WTP, (B) UV/$NH_2Cl$ disinfection, Lovö WTP and (C) $NH_2Cl$/UV disinfection, Kvarnagården WTP. (For interpretation of the references to color in this figure legend, the reader is referred to the web version of this article.)

TotAbs/DOC, TotFDOM/DOC, and SUVA (Table 1). However, when plotting the differential absorbance, the shoulder commonly present for DOM around 260–270 nm (Korshin et al., 1997) appeared to have been particularly susceptible to the treatment over the entire sampling period (Fig. A6). The effect of slow sand filtration on FDOM was opposite to coagulation with the largest removal of components emitting at relatively short wavelengths (Fig. 1). The same pattern was seen for all sampling occasions where removal of FDOM was quantifiable. Accordingly, this treatment resulted in an increase in $\%FDOM_{450\text{-}600}$, and a decrease in β:α (Table 1). Opposite to coagulation, FI obtained from ΔEEMs (1.70 ± 0.10) was close to a microbially derived end member (approximately 1.8) (Cory and McKnight, 2005; Cory et al., 2007; McKnight et al., 2001), while HIX was low (0.82 ± 0.02) and β:α high (0.98 ± 0.10) compared to FDOM removed during coagulation (Fig. 4). The largest removal of FDOM and CDOM (Fig. 1 & A6) overlapped with the emission of tryptophan, tyrosine and phenylalanine (Coble, 1996; Coble et al., 1990; Lakowicz, 2007). This FDOM is generally referred to as protein-like and is thought to represent free or bound amino acids (Coble, 1996; Coble et al., 1998, 1990; Parlanti et al., 2000), mainly of autochthonous origin. With rank correlation we showed that in-lake produced FDOM correlated with CHO components having negative average carbon oxidation state ($\overline{C_{OS}} \leq 0$, Fig. 3), which should, consequently, have been particularly susceptible to removal due to the preferential removal of FDOM with emission between 300 and 450 nm (Fig. 1). Differential EEMs showed that, in addition to protein-like FDOM, of which 15 ± 4% (average ± standard deviation over time, $p < 0.001$) was removed at an excitation/emission wavelength pair of 275/320 nm during the sampled period, approximately 5% of FDOM with longer emission wavelengths (Em > 450 nm) (6 ± 2% (average ± standard deviation over time) at excitation = 350 nm and emission = 548 nm, $p < 0.001$) could be removed during slow sand filtration (Fig. 1). The net DOM removal during slow sand filtration is the sum of uptake and production of DOM by microbial biofilms, as well as physical retention, and may vary among WTPs in response to the composition of DOM as well as of microbial communities. Also, within the protein-like FDOM, different components may be removed by biofilms to a varying extent (Cory and Kaplan, 2012).

### 3.2.3. Disinfection

DOC concentration and spectroscopic parameters did not change significantly during disinfection at neither Lovö nor Kvarnagården WTPs (Table 1). Still, differential absorbance curves revealed that CDOM absorbing at 260–270 nm was most reactive during disinfection (Fig. A6), which is consistent with earlier studies (Korshin et al., 2002; Roccaro and Vagliasindi, 2009). The removal of CDOM was very similar for disinfection and slow sand filtration (Fig. A6). Due to this similarity and because protein-like FDOM was particularly reactive during slow sand filtration, this material is likely to have caused consumption of the disinfectant, even if no significant changes in fluorescence properties could be quantified during disinfection. Removal of in-lake produced FDOM prior to disinfection (as occurs both during slow sand filtration and coagulation) should therefore be beneficial in order to lower the unwanted consumption of disinfectants by DOM. As previously reported, we observed a general shift from reduced to oxidized components during disinfection, demonstrated with increasing weighted mean values of the average carbon oxidation state (Lavonen et al., 2013). In this study, we have investigated this on a single component basis and observed that, at both WTPs, practically all components that decreased in relative abundance with more than 2.5 percentage points during disinfection were reduced ($\overline{C_{OS}} \leq 0$) (Fig. 3, Tables A6 and A7). Similarly, Zhang et al. (2012a) found that components with low O/C were especially reactive towards chlorine, as expected due to the larger energy gained for oxidation of the most reduced molecule. Out of the CHO components that decreased significantly the larger majority were correlated to in-lake produced DOM at both WTPs (58 and 67% at Lovö and Kvarnagården WTPs respectively), while none correlated with terrestrial DOM (Tables A6 & A7). Beggs and Summers (2011) also found that protein-like FDOM components were especially reactive during chlorination and caused the majority of chlorine consumption, however using pine needle leachates. They further concluded that humic-like FDOM was more prone to form chlorine-containing disinfection by-products measured as trihalomethanes and haloacetic acids. Similarly, others have found that hydrophobic, aromatic compounds with oxygen functional groups are the most potent precursors for chlorine-containing disinfection by-products (Croué et al., 2000; Lavonen et al., 2013; Rook, 1977). At Kvarnagården WTP, the shift in DOM composition during disinfection was more pronounced than at Lovö (Fig. 5B&C), which may be connected to a larger $NH_2Cl$ consumption (Lavonen et al., 2013). Nevertheless, this difference could not be related to a larger fraction of in-lake produced DOM present before disinfection, as could be expected. Instead, at Kvarnagården β:α and FI were significantly lower and $\%FDOM_{450\text{-}600}$ and SUVA markedly higher before disinfection than at Lovö. Factors other than the DOM composition that might have affected the $NH_2Cl$ consumption were the approximately 70% higher dose per DOC at Kvarnagården (Lavonen et al., 2013) and that UV treatment was applied before $NH_2Cl$ at Lovö while the processes were in reversed order at Kvarnagården WTP. Applying UV disinfection could have oxidized the CHO components to an extent lowering $NH_2Cl$ consumption at Lovö WTP while still not oxidizing the components as extensively as during the $NH_2Cl$/UV treatment at Kvarnagården WTP, but that cannot be assessed from our data. Clearly, further studies under more controlled conditions are needed to identify parameters that can be used to explain disinfectant consumption and the extent of CHO component oxidation during disinfection. The shift from reduced to oxidized CHO formulas during disinfection indicates that in-lake produced DOM was especially reactive during disinfection and responsible for the largest consumption of disinfectant, but likely to mainly have resulted in the formation of oxidized, non-chlorinated by-products.

## 3.3. DOM treatability

In order to explain differences in treatability of raw waters in a simple and straight-forward manner, we used the specific spectral characteristics associated with DOC removal efficiency described above in Section 3.2. The total DOC removal varied widely from 74 ± 3% at Ringsjö, 53 ± 3% at Lackarebäck and 49 ± 3% at Lovö to no quantifiable loss at Kvarnagården WTP. Differential EEMs were especially useful to describe selective removal of FDOM during coagulation and slow sand filtration, because the reactivity of both terrestrial and in-lake produced DOM can be obtained simultaneously (see Section 3.2). We suggest that by comparing different waters using normalized ΔEEMs their relative treatability can be assessed. By normalizing the data before calculation of ΔEEMs we obtain a direct comparison of the DOM quality in two samples containing different amounts of fluorescent DOM. The difference in total DOC removal, of which the majority occurred during coagulation, was evident when comparing normalized ΔEEMs of raw waters from Ringsjö with Lovö and Lackarebäck WTPs over the entire sampling period, as exemplified in Fig. 6. The FDOM in raw waters of Lovö and Lackarebäck differed from that of Ringsjö WTP, with large differences in DOC reduction attributed to a larger abundance of more easily coagulated FDOM in Ringsjö WTP raw water. The differences in FDOM composition between the raw

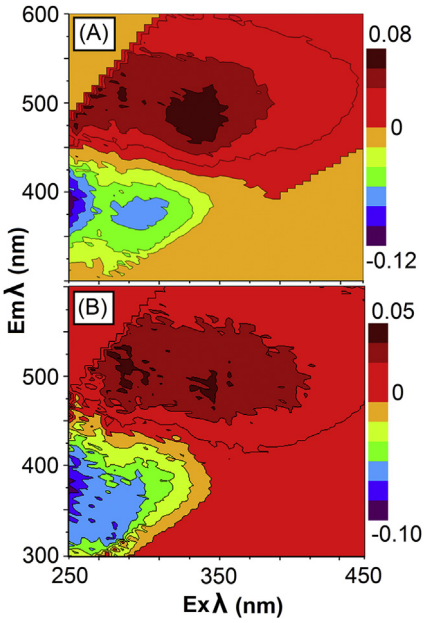


**Fig. 6.** Normalized differential EEMs for raw waters from (A) Ringsjö water treatment plant (WTP) compared with Lovö WTP and (B) Ringsjö WTP compared with Lackarebäck WTP (2011-10-18). Values above zero demonstrate fluorescing dissolved organic matter (FDOM) representing a larger fraction of the total FDOM at Ringsjö and values below zero FDOM that occurred more (to a relative extent) in Lovö/Lackarebäck WTPs raw water.

waters corresponded to the change occurring at Lovö WTP during coagulation (compare Figs. 1 and 6). We argue that normalized ΔEEMs demonstrate a more complete picture of differences in the DOM composition of two samples compared to SUVA and the fluorescence indices by visualizing the relative contributions of different fluorophores simultaneously.

Highly detailed information regarding treatability of DOM can be obtained with advanced analytical techniques such as the FT-ICR-MS employed in this study. However, using differential EEMs we have demonstrated that the relative treatability of two different waters can be assessed in a simple and straightforward way that should be attractive to use at WTPs, where time and resources may limit the feasibility of advanced methods (e.g. FT-ICR-MS) and data treatment (e.g., parallel factor analysis (PARAFAC) which is commonly applied to EEMs). We therefore recommend WTPs to use differential EEMs to assess the process-specific selective removal of FDOM. Differential EEMs could also be used to compare the DOM quality in different water sources and could be used to carefully monitor treatability over time, and be of great aid when investigating alternative treatment processes, raw water sources or intake depths.

## 4. Conclusions

Using a combination of bulk (DOC), optical (absorbance and fluorescence) and molecular level (FT-ICR-MS) analytical tools to assess the reactivity of DOM during conventional drinking water treatment, the following conclusions could be drawn:

- All the investigated drinking water treatment processes targeted specific fractions of DOC. When DOC removal was low (i.e. during slow sand filtration and disinfection) this could not be detected with the commonly used parameter SUVA, but was clear from differential fluorescence and absorbance measurements or FT-ICR-MS analyzes.
- Differential EEMs were especially useful to assess DOM reactivity as a range of removal efficiencies for both terrestrial and in-lake produced DOM can be obtained simultaneously, compared to established indices where only information regarding the most reactive end-member is given.
- We used rank correlation to couple spectroscopic parameters to specific chemical components obtained with FT-ICR-MS analyzes. The rank correlation divided the spectroscopic indices into two groups which corresponded to commonly known DOM, namely terrestrial (represented by high HIX, SUVA and %$FDOM_{450-600}$), and in-lake produced DOM (represented by high β:α, FI and %$FDOM_{300-450}$). The most striking difference between chemical formulas correlated to the optical parameters in the two groups was the average carbon oxidation state that was $\geq$0 for components correlated with terrestrial DOM and $\leq$0 for those coupled to in-lake produced DOM.
- The average carbon oxidation state was an important factor differentiating between components prone to removal by coagulation (oxidized) and slow sand filtration (reduced) as well as those consuming disinfectant (reduced) and acting as precursors for disinfection by-products (oxidized).

## Acknowledgments

We would like to thank the personnel at the four water treatment plants for assistance with sampling and Jan Johansson at Uppsala University for performing the absorbance and fluorescence measurements. This work was funded by The Swedish Research Council Formas, 219-2009-1692 through the strong research environment Color of Water (CoW). This is contribution 5079 of the University of Maryland Center for Environmental Science.

## Appendix A. Supplementary data

Supplementary data related to this article can be found at http://dx.doi.org/10.1016/j.watres.2015.08.024.

## References

Baghoth, S., Sharma, S., Amy, G., 2011. Tracking natural organic matter (NOM) in a drinking water treatment plant using fluorescence excitation–emission matrices and PARAFAC. Water Res. 45 (2), 797–809.
Bieroza, M., Baker, A., Bridgeman, J., 2009a. Exploratory analysis of excitation-emission matrix fluorescence spectra with self-organizing maps as a basis for determination of organic matter removal efficiency at water treatment works. J. Geophys. Res. Biogeosci. (2005–2012) 114 (G4).
Bieroza, M., Baker, A., Bridgeman, J., 2009b. Relating freshwater organic matter fluorescence to organic carbon removal efficiency in drinking water treatment. Sci. total Environ. 407 (5), 1765–1774.
Bieroza, M., Baker, A., Bridgeman, J., 2010. Fluorescence spectroscopy as a tool for determination of organic matter removal efficiency at water treatment works. Drink. Water Eng. Sci. 3 (1), 63–70.
Camper, A.K., 2004. Involvement of humic substances in regrowth. Int. J. Food Microbiol. 92 (3), 355–364.
Coble, P.G., 1996. Characterization of marine and terrestrial DOM in seawater using excitation emission matrix spectroscopy. Mar. Chem. 51 (4), 325–346.
Coble, P.G., Green, S.A., Blough, N.V., Gagosian, R.B., 1990. Characterization of Dissolved Organic Matter in the Black Sea by Fluorescence Spectroscopy.
Coble, P.G., Del Castillo, C.E., Avril, B., 1998. Distribution and optical properties of CDOM in the Arabian Sea during the 1995 southwest monsoon. Deep-Sea Res. Part II 45 (10–11), 2195–2223.
Cory, R.M., Kaplan, L.A., 2012. Biological lability of streamwater fluorescent dissolved organic matter. Limnol. Oceanogr. 57 (5), 1347.
Cory, R.M., McKnight, D.M., 2005. Fluorescence spectroscopy reveals ubiquitous presence of oxidized and reduced quinones in dissolved organic matter. Environ. Sci. Technol. 39 (21), 8142–8149.
Cory, R.M., McKnight, D.M., Chin, Y.P., Miller, P., Jaros, C.L., 2007. Chemical characteristics of fulvic acids from Arctic surface waters: microbial contributions and photochemical transformations. J. Geophys. Res. Biogeosci. (2005–2012) 112 (G4).
Croué, J.-P., Violleau, D., Labouyrie, L., 2000. Natural Organic Matter and Disinfection By-products, pp. 139–153 (ACS Symposium Series).
Dittmar, T., Koch, B., Hertkorn, N., Kattner, G., 2008. A simple and efficient method for the solid-phase extraction of dissolved organic matter (SPE-DOM) from

seawater. Limnol. Oceanogr. Methods 6, 230–235.
Edzwald, J., 1993. Coagulation in drinking water treatment: particles, organics and coagulants. Water Sci. Technol. 27 (11), 21–35.
Eikebrokk, B., Vogt, R.D., Liltved, H., 2004. NOM increase in Northern European source waters: discussion of possible causes and impacts on coagulation/contact filtration processes. Water Sci. Technol. 4 (4), 47–54.
Evans, C.D., Monteith, D.T., Cooper, D.M., 2005. Long-term increases in surface water dissolved organic carbon: observations, possible causes and environmental impacts. Environ. Pollut. 137, 55–71.
Freeman, C., Evans, C.D., Monteith, D.T., 2001. Export of organic carbon from peat soils. Nature 412, 785.
Gonsior, M., Zwartjes, M., Cooper, W., Song, W., Ishida, K., Tseng, L., Jeung, M., Rosso, D., Hertkorn, N., Schmitt-Kopplin, P., 2011. Molecular characterization of effluent organic matter identified by ultrahigh resolution mass spectrometry. Water Res. 45 (9), 2943–2953.
Gonsior, M., Schmitt-Kopplin, P., Bastviken, D., 2013. Depth-dependent molecular composition and photo-reactivity of dissolved organic matter in a boreal lake under winter and summer conditions. Biogeosciences 10 (11), 6945–6956.
Gonsior, M., Schmitt-Kopplin, P., Stavklint, H., Richardson, S.D., Hertkorn, N., Bastviken, D., 2014. Changes in dissolved organic matter during the treatment processes of a drinking water plant in Sweden and formation of previously unknown disinfection byproducts. Environ. Sci. Technol. 48 (21), 12714–12722.
Herzsprung, P., von Tumpling, W., Hertkorn, N., Harir, M., Buttner, O., Bravidor, J., Friese, K., Schmitt-Kopplin, P., 2012. Variations of DOM quality in inflows of a drinking water reservoir: linking of van Krevelen diagrams with EEMF spectra by rank correlation. Environ. Sci. Technol. 46 (10), 5511–5518.
Hongve, D., Riise, G., Kristiansen, J.F., 2004. Increased colour and organic acid concentrations in Norwegian forest lakes and drinking water–a result of increased precipitation? Aquat. Sci. 66 (2), 231–238.
Huck, P.M., 1990. Measurement of biodegradable organic matter and bacterial growth potential in drinking water. J. Am. Water Works Assoc. 82 (7), 78–86.
Kaiya, Y., Itoh, Y., Fujita, K., Takizawa, S., 1996. Study on fouling materials in the membrane treatment process for potable water. Desalination 106 (1–3), 71–77.
Kellerman, A.M., Dittmar, T., Kothawala, D.N., Tranvik, L.J., 2014. Chemodiversity of dissolved organic matter in lakes driven by climate and hydrology. Nat. Commun. 5.
Kleber, M., Johnson, M.G., 2010. Advances in understanding the molecular structure of soil organic matter: implications for interactions in the environment. Adv. Agron. 106, 77–142.
Korshin, G.V., Li, C.-W., Benjamin, M.M., 1997. Monitoring the properties of natural organic matter through UV spectroscopy: a consistent theory. Water Res. 31 (7), 1787–1795.
Korshin, G.V., Wu, W.W., Benjamin, M.M., Hemingway, O., 2002. Correlations between differential absorbance and the formation of individual DBPs. Water Res. 36 (13), 3273–3282.
Kothawala, D.N., Murphy, K.R., Stedmon, C.A., Weyhenmeyer, G.A., Tranvik, L.J., 2013. Inner filter correction of dissolved organic matter fluorescence. Limnol. Oceanogr. Methods 11, 616–630.
Kothawala, D.N., Stedmon, C.A., Müller, R.A., Weyhenmeyer, G.A., Köhler, S.J., Tranvik, L.J., 2014. Controls of dissolved organic matter quality: evidence from a large-scale boreal lake survey. Glob. Change Biol. 20 (4), 1101–1114.
Kroll, J.H., Donahue, N.M., Jimenez, J.L., Kessler, S.H., Canagaratna, M.R., Wilson, K.R., Altieri, K.E., Mazzoleni, L.R., Wozniak, A.S., Bluhm, H., Mysak, E.R., Smith, J.D., Kolb, C.E., Worsnop, D.R., 2011. Carbon oxidation state as a metric for describing the chemistry of atmospheric organic aerosol. Nat. Chem. 3 (2), 133–139.
Lakowicz, J.R., 2007. Principles of Fluorescence Spectroscopy. Springer.
Lavonen, E.E., Gonsior, M., Tranvik, L.J., Schmitt-Kopplin, P., Köhler, S.J., 2013. Selective chlorination of natural organic matter: identification of previously unknown disinfection byproducts. Environ. Sci. Technol. 47 (5), 2264–2271.
Lawaetz, A.J., Stedmon, C.A., 2009. Fluorescence intensity calibration using the Raman scatter peak of water. Appl. Spectrosc. 63 (8), 936–940.
Ledesma, J.L., Köhler, S.J., Futter, M.N., 2012. Long-term dynamics of dissolved organic carbon: implications for drinking water supply. Sci. total Environ. 432, 1–11.
Liu, C., Tang, X., Kim, J., Korshin, G.V., 2015. Formation of aldehydes and carboxylic acids in ozonated surface water and wastewater: a clear relationship with fluorescence changes. Chemosphere 125, 182–190.
MacDonald, B.C., Lvin, S.J., Patterson, H., 1997. Correction of fluorescence inner filter effects and the partitioning of pyrene to dissolved organic carbon. Anal. Chim. Acta 338 (1), 155–162.
Matilainen, A., Vepsalainen, M., Sillanpaa, M., 2010. Natural organic matter removal by coagulation during drinking water treatment: a review. Adv. Colloid Interface Sci. 159 (2), 189–197.
Matilainen, A., Gjessing, E.T., Lahtinen, T., Hed, L., Bhatnagar, A., Sillanpaa, M., 2011. An overview of the methods used in the characterisation of natural organic matter (NOM) in relation to drinking water treatment. Chemosphere 83 (11), 1431–1442.
McKnight, D.M., Boyer, E.W., Westerhoff, P.K., Doran, P.T., Kulbe, T., Andersen, D.T., 2001. Spectrofluorometric characterization of dissolved organic matter for indication of precursor organic material and aromaticity. Limnol. Oceanogr. 46 (1), 38–48.
Ødegaard, H., Østerhus, S., Melin, E., Eikebrokk, B., 2010. NOM removal technologies–Norwegian experiences. Drink. Water Eng. Sci. 3 (1), 1–9.
Ohno, T., 2002. Fluorescence inner-filtering correction for determining the humification index of dissolved organic matter. Environ. Sci. Technol. 36 (4), 742–746.
Parlanti, E., Wörz, K., Geoffroy, L., Lamotte, M., 2000. Dissolved organic matter fluorescence spectroscopy as a tool to estimate biological activity in a coastal zone submitted to anthropogenic inputs. Org. Geochem. 31 (12), 1765–1781.
Richardson, S.D., 2011. Disinfection by-products: formation and occurrence in drinking water (Chapter 2). In: Nriagu, J.O. (Ed.), Encyclopedia of Environmental Health, vol. 2. Elsevier Science Inc., Burlington, MA, pp. 110–136.
Richardson, S.D., Plewa, M.J., Wagner, E.D., Schoeny, R., DeMarini, D.M., 2007. Occurrence, genotoxicity, and carcinogenicity of regulated and emerging disinfection by-products in drinking water: a review and roadmap for research. Mutat. Res. – Rev. Mutat. Res. 636 (1–3), 178–242.
Roccaro, P., Vagliasindi, F.G., 2009. Differential vs. absolute UV absorbance approaches in studying NOM reactivity in DBPs formation: comparison and applicability. Water Res. 43 (3), 744–750.
Roccaro, P., Vagliasindi, F.G., Korshin, G.V., 2009. Changes in NOM fluorescence caused by chlorination and their associations with disinfection by-products formation. Environ. Sci. Technol. 43 (3), 724–729.
Rook, J.J., 1977. Chlorination reactions of fulvic acids in natural waters. Environ. Sci. Technol. 11 (5), 478–482.
Roulet, N., Moore, T.R., 2006. Browning the waters. Nature 444, 283–284.
Sanchez, N.P., Skeriotis, A.T., Miller, C.M., 2013. Assessment of dissolved organic matter fluorescence PARAFAC components before and after coagulation–filtration in a full scale water treatment plant. Water Res. 47 (4), 1679–1690.
Savitzky, A., Golay, M.J., 1964. Smoothing and differentiation of data by simplified least squares procedures. Anal. Chem. 36 (8), 1627–1639.
Senesi, N., 1990. Molecular and quantitative aspects of the chemistry of fulvic acid and its interactions with metal ions and organic chemicals: Part II. The fluorescence spectroscopy approach. Anal. Chim. Acta 232, 77–106.
Shutova, Y., Baker, A., Bridgeman, J., Henderson, R.K., 2014. Spectroscopic characterisation of dissolved organic matter changes in drinking water treatment: from PARAFAC analysis to online monitoring wavelengths. Water Res. 54 (0), 159–169.
Steinberg, C.E., Meinelt, T., Timofeyev, M.A., Bittner, M., Menzel, R., 2008. Humic substances. Environ. Sci. Pollut. Res. 15 (2), 128–135.
Stubbins, A., Lapierre, J.-F., Berggren, M., Prairie, Y., Dittmar, T., del Giorgio, P., 2014. What's in an EEM? Molecular signatures associated with dissolved organic fluorescence in Boreal Canada. Environ. Sci. Technol. 48 (18), 10598–10606.
Summers, R.S., Haist, B., Koehler, J., Ritz, J., Zimmer, G., Sontheimer, H., 1989. The influence of background organic matter on GAC adsorption. Am. Water Works Assoc. J. 81 (5), 66–74.
Thurman, E.M., 1985. Organic Geochemistry of Natural Waters. Springer.
Traina, S.J., Novak, J., Smeck, N.E., 1990. An ultraviolet absorbance method of estimating the percent aromatic carbon content of humic acids. J. Environ. Qual. 19 (1), 151–153.
Volk, C., Bell, K., Ibrahim, E., Verges, D., Amy, G., LeChevallier, M., 2000. Impact of enhanced and optimized coagulation on removal of organic matter and its biodegradable fraction in drinking water. Water Res. 34 (12), 3247–3257.
Weishaar, J.L., Aiken, G.R., Bergamaschi, B.A., Fram, M.S., Fujii, R., Mopper, K., 2003. Evaluation of specific ultraviolet absorbance as an indicator of the chemical composition and reactivity of dissolved organic carbon. Environ. Sci. Technol. 37 (20), 4702–4708.
Zhang, H., Zhang, Y., Shi, Q., Ren, S., Yu, J., Ji, F., Lou, W., Yang, M., 2012a. Characterization of low molecular weight dissolved natural organic matter along the treatment trait of a waterworks using Fourier transform ion cyclotron resonance mass spectrometry. Water Res. 5197–5204.
Zhang, H.F., Zhang, Y.H., Shi, Q., Hu, J.Y., Chu, M.Q., Yu, J.W., Yang, M., 2012b. Study on transformation of natural organic matter in source water during chlorination and its chlorinated products using ultrahigh resolution mass spectrometry. Environ. Sci. Technol. 46 (8), 4396–4402.
Zsolnay, A., Baigar, E., Jimenez, M., Steinweg, B., Saccomandi, F., 1999. Differentiating with fluorescence spectroscopy the sources of dissolved organic matter in soils subjected to drying. Chemosphere 38 (1), 45–50.